Stimulation of CD95 (Fas) blocks T lymphocyte calcium channels through sphingomyelinase and sphingolipids

Albrecht Lepple-Wienhues*†, Claus Belka‡, Tilmann Laun*, Andreas Jekle*, Birgit Walter*, Ulrich Wieland*, Martina Welz*, Luzia Heil*, Jutta Kun*, Gillian Busch*, Michael Weller§, Michael Bamberg‡, Erich Gulbins*¶, and Florian Lang*¶

Departments of *Physiology I, ‡Radiooncology, and §Neurology, University of Tübingen, Gmelinstr. 5, D-72076 Tübingen, Germany

Edited by Bertil Hille, University of Washington, Seattle, WA, and approved August 26, 1999 (received for review April 5, 1999)

Calcium influx through store-operated calcium release-activated calcium channels (CRAC) is required for T cell activation, cytokine synthesis, and proliferation. The CD95 (Apo-1/Fas) receptor plays a role in self-tolerance and tumor immune escape, and it mediates apoptosis in activated T cells. In this paper we show that CD95-stimulation blocks CRAC and Ca^{2+} influx in lymphocytes through the activation of acidic sphingomyelinase (ASM) and ceramide release. The block of Ca^{2+} entry is lacking in CD95-defective *lpr* lymphocytes as well as in ASM-defective cells and can be restored by retransfection of ASM. C2 ceramide, C6 ceramide, and sphingosine block CRAC reversibly, whereas the inactive dihydroceramide has no effect. CD95-stimulation or the addition of ceramide prevents store-operated Ca^{2+} influx, activation of the transcriptional regulator NFAT, and IL-2 synthesis. The block of CRAC by sphingomyelinase metabolites adds a function to the repertoire of the CD95 receptor inhibiting T cell activation signals.

Store-operated Ca^{2+} entry mediated by calcium release-activated calcium channels (CRAC) is important for many lymphocyte functions, including proliferation, cytokine generation, and differentiation (reviewed in ref. 1). Stimulation of the T cell receptor (TCR) complex generates inositoltrisphosphate, which releases Ca^{2+} from endoplasmic reticulum stores. The reduced Ca^{2+} content of these stores then opens CRAC, leading to a sustained Ca^{2+} influx (2). In T cells, a lasting Ca^{2+} rise >500 nM is required to induce IL-2 synthesis (3). The inhibition of Ca^{2+}-dependent signaling pathways with cyclosporin or ion channel blockers completely suppresses T cell activation (reviewed in ref. 4).

The CD95-receptor induces apoptosis in lymphocytes and is critically involved in the maintenance of self-tolerance (reviewed in ref. 5). Expression of the CD95 ligand (CD95L) can create immune privileged sites (6, 7), and malignant tumors may escape from the immune attack by expressing high levels of CD95L (8, 9).

However, CD95 may have additional functions apart from lymphocyte apoptosis. First, freshly activated T lymphocytes express CD95 but are resistant to CD95-mediated apoptosis (10, 11). Second, in tumor patients, defective lymphocyte function rather than apoptotic deletion has been observed (12, 13). Third, mice inoculated with a CD95L-expressing tumor develop severe CD95-mediated defects in lymphocyte function (14). Fourth, the knockout of CD95-activated signaling molecules required for apoptosis does not, in contrast to CD95-knockout, result in lymphoproliferative disease (15, 16). Thus, apoptosis may not represent the only function of CD95 in immune tolerance.

Materials and Methods

Cells. Jurkat T cells, Niemann–Pick Disease type A (NPDA), Daudi, and JY B cells were maintained in RPMI medium 1640, and LN18 and LN229 glioblastoma were maintained in DMEM (17). The stimulating monoclonal mouse anti-human CD95 (CH11; Upstate Biotechnology, Lake Placid, NY) was added at 100 ng/ml. Apoptosis was assayed by nuclear fragmentation (Hoe33342, propidium iodide or SYTO 16; Molecular Probes) or FITC-annexin flow cytometry. Peripheral T lymphoblasts were prepared by using a Ficoll gradient, purified with nylon wool columns (>90% $CD3^+$), and stimulated with 1 μg/ml phythaemaglutinin (PHA) (24 h) plus 2.5 units/ml IL-2 (4–6 days). Thymocytes were prepared from homozygous C57/Bl6 *lpr*- and *gld* mice (ages 10–15 weeks). Transient transfection of NPDA cells was performed by electroporation with an expression vector encoding acidic sphingomyelinase (ASM) (pJK-*asm,* 15 μg/ml) and a *Myc*-tagged single chain (18). Twelve hours after electroporation viable cells were purified by Ficoll gradient centrifugation and cultured for an additional 24 h. After 36 h, Myc presented on the cell surface was stained with a monoclonal anti-*Myc*-antibody (9E10; American Type Culture Collection, Bethesda, MD) and a phycoerythrin-conjugated secondary antibody (18) for the identification of transfected cells yielding a transfection efficiency of 25–30%.

Patch-Clamp Recordings. Whole-cell currents were recorded with an EPC-9 patch-clamp amplifier (HEKA Electronics, Lambrecht/Pfalz, Germany) at 20°C. Data were sampled at 5 kHz and digitally filtered at 0.5 kHz for analysis and display. Capacitive transients were canceled and voltage was corrected for liquid junction potentials. The pipette contained 128 mM cesium aspartate, 10 mM Hepes (pH 7.2), 12 mM EGTA, 0.7 mM $CaCl_2$, and 3.0 mM $MgCl_2$ (10 nM free $[Ca^{2+}]$). Extracellular solutions contained 145 mM NaCl, 5 mM KCl, 2 mM $CaCl_2$, 1 mM $MgCl_2$, 10 mM glucose, and 10 mM Hepes (pH 7.4). For experiments with sphingolipids 0.1% BSA was added to all solutions.

Intracellular Free Ca^{2+} Concentration ($[Ca^{2+}]_i$) Measurements. Flow cytometric analysis (FACS Calibur, Becton Dickinson, excitation 488 nm) of $[Ca^{2+}]_i$ was performed in single cells after loading at 37°C with 4.5 μM of fura-red-acetoxymethyl ester for 30 min and 0.5 μM of fluo-3-acetoxymethyl ester for 10 min in the presence of 0.015% pluronic acid (Molecular Probes). Calibration was performed for each experimental condition by using 10 μM ionomycin and varying external Ca^{2+} concentrations. Ca^{2+} concentrations were approximated as described (19) and confirmed with fura-2 fluorescence microscopy. For digital ratiometric fluorescence microscopy, cells were loaded at 37°C with fura-2-acetoxymethyl ester (Molecular Probes) on glass coverslips coated with poly-L-lysine. Digital video imaging ratios (340:380 nm excitation and 510 nm emission) were obtained on

This paper was submitted directly (Track II) to the PNAS office.

Abbreviations: CD95L, CD95 ligand; ASM, acidic sphingomyelinase; CRAC, calcium release-activated calcium channels; $[Ca^{2+}]_i$, intracellular Ca^{2+} concentration; TG, thapsigargin; NPDA, Niemann–Pick Disease type A; TCR, T cell receptor; PHA, phythaemaglutinin.

†To whom reprint requests should be addressed. E-mail: alepplew@uni-tuebingen.de.

¶E.G. and F.L. contributed equally to this work.

The publication costs of this article were defrayed in part by page charge payment. This article must therefore be hereby marked "*advertisement*" in accordance with 18 U.S.C. §1734 solely to indicate this fact.

a Zeiss Axiovert 135 fluorescence microscope at 34°C, recorded with an intensified charge-coupled device camera, and digitized with an Axon image lightning system (Axon Instruments, Foster City, CA). *In situ* calibration was performed as described above.

IL-2 Assay. Intracellular IL-2 content was analyzed by FACS. Cytokine release was blocked by monensin (1 μM). Cells were stimulated with 50 μg/ml PHA and 100 nM phorbol 12-myristate 13-acetate for 5 h, fixed, permeabilized (Cytofix/Cytoperm, PharMingen), and stained with a FITC-conjugated rat anti-human IL-2 IgG2a or matched isotype control antibody (1.5 μg/ml, PharMingen). Apoptotic cells were excluded by gating.

Gel Mobility Shift Assays of NFAT. Cells were stimulated with 1 μM of thapsigargin (TG) for 20 min; 100 ng/ml CD95-antibody was added at 1 h, 400 nM cyclosporin A at 2 h before, and 100 μM C2 ceramide simultaneously with TG. Cells were then incubated for 1 h in 10 mM Hepes, pH 7.9/10 mM KCl/0.01 mM EDTA/0.01 mM EGTA/20 mM PMSF/1 mM DTT (buffer A) at 0°C. Nonidet P-40 (0.6%) was added, nuclei were pelleted and washed in buffer A, and nuclear proteins were eluted for 1 h in 20 mM Hepes, pH 7.9/400 mM KCl/0.1 mM EDTA/20 mM PMSF/1 mM DTT/10% glycerol. DNA consensus nucleotides (NFATc: GGAAAA, and AP-1: TGACTCA) (Santa Cruz Biotechnology) matching the NFAT binding sequence in the IL-2 promoter were ^{32}P-labeled with T4 polynucleotide kinase (Promega). Gel mobility shifts were electrophoretically separated by PAGE in 0.5× TBE buffer (90 mM Tris/64.6 mM boric acid/2.5 mM EDTA, pH 8.3) and analyzed by autoradiography.

Measurement of Cellular Ceramide. Cells (5×10^6) were stimulated with 100 ng/ml CH11 antibody. Lipids were extracted in $CHCl_3$:CH_3OH:1M HCl (100:100:1), dried, dissolved, and 40 μg/ml purified diacylglycerol kinase, 10 μCi per sample [γ-^{32}P]ATP, and 5 mM ATP were added. After 30 min at 20°C, the reaction was stopped by the addition of 1 ml of $CHCl_3$:CH_3OH:1M HCl (100:100:1), 170 μl of extracellular solution, and 30 μl of 100 mM EDTA. The lower organic phase was dried and resuspended in $CHCl_3$:CH_3OH (1:1), and lipids were separated by TLC with $CHCl_3$:CH_3OH:acetic acid (13:3:1) as solvent. Spots were visualized by autoradiography, cut out, and analyzed by liquid scintillation counting. Uptake of extracellularly applied ^{14}C-labeled C2 ceramide (1 μCi per sample; American Radiolabeled Chemicals Inc., St. Louis) was studied by using 10^6 cells in 1 ml of extracellular solution containing 0.1% BSA. After a 5-min incubation at 20°C, the cells were washed three times in fresh vials and activity was counted.

Results

CD95-Stimulation Blocks Ca^{2+} Entry in Human T Lymphocytes. To analyze CD95 effects on Ca^{2+} signals in human peripheral T cells, $[Ca^{2+}]_i$ was measured in single lymphoblasts (Fig. 1). After 24 h of CD95-stimulation, store-operated Ca^{2+} entry was inhibited in viable cells (Fig. 1 *C* and *D*). TG was used to activate store-operated Ca^{2+} entry, because it specifically blocks the endoplasmic Ca^{2+} pump leading to maximal activation of store-operated Ca^{2+} channels (20). Even resting calcium levels were slightly reduced following CD95 stimulation (not shown). In contrast to store-operated Ca^{2+} entry, permeabilizing the cells with 10 μM ionomycin increased $[Ca^{2+}]_i$ whether CD95 was triggered or not (Fig. 1 *E* and *F*).

We then investigated the time course of Ca^{2+} entry after CD95 stimulation. The block of TG-induced Ca^{2+} influx following CD95 stimulation was already seen after 1 h in human peripheral T lymphoblasts and Jurkat T cells (Fig. 1*G*) and lasted for >18 h. The same result was obtained when Ca^{2+} influx was stimulated via the TCR (10 μg/ml PHA, not shown). The

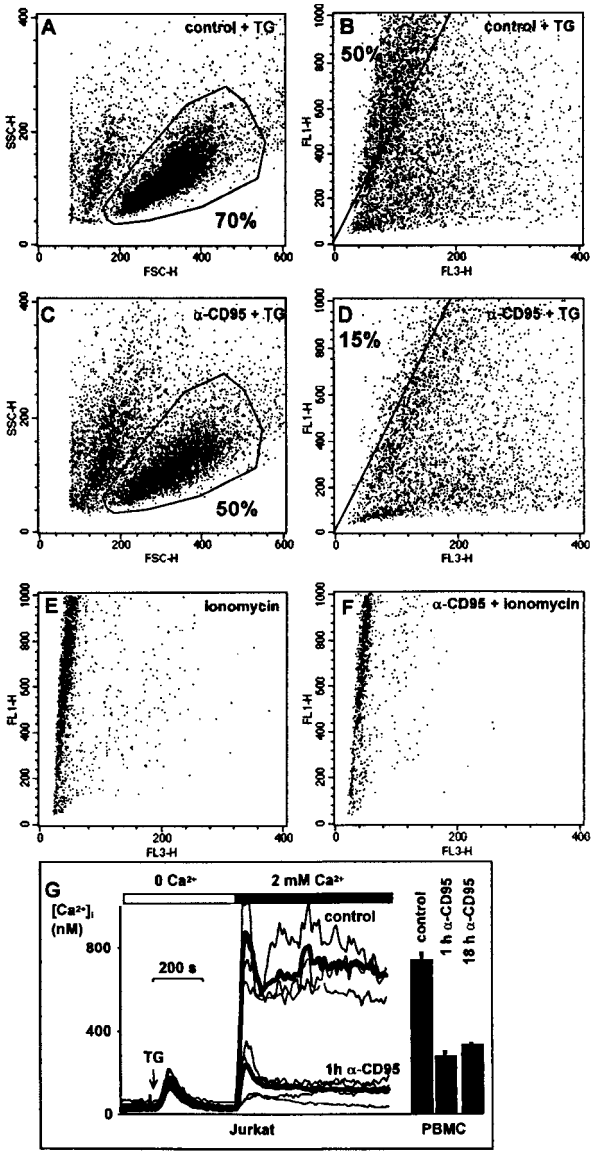

Fig. 1. Block of store-operated Ca^{2+} entry in apoptosis-resistant T lymphocytes by CD95 stimulation. (*A*) Forward/sideward scatter plots indicate ≈70% viable human peripheral lymphoblasts after 5-day culture in 2.5 units/ml IL-2. In *A–F* viable cells were gated and used for $[Ca^{2+}]_i$ analysis by using flow cytometry. (*B*) FL1/FL3 fluorescence ratios indicate intracellular Ca^{2+} levels in single viable cells. When store-operated Ca^{2+} entry is stimulated with 1 μM TG, 50% of the cells show a FL1/FL3 ratio exceeding ≈500 nM $[Ca^{2+}]_i$. (*C*) Cells were exposed to CD95 antibody (100 ng/ml) for 24 h. Fifty percent of the cells are resistant to apoptosis as confirmed by propidium iodide staining (not shown). (*D*) Store-operated Ca^{2+} entry is inhibited in apoptosis-resistant lymphoblasts after CD95 stimulation indicated by the low FL1/FL3 ratio. Only 15% of the population exceed ≈500 nM $[Ca^{2+}]_i$ when stimulated with TG. (*E*) Maximal FL1/FL3 ratio is obtained with 10 μM ionomycin and 2 mM extracellular Ca^{2+}. (*F*) The elevation of $[Ca^{2+}]_i$ by 10 μM ionomycin is not affected by CD95. (*G*) Block of store-operated Ca^{2+} influx in Jurkat T cells and peripheral lymphoblasts is an early and lasting event after CD95 stimulation. This panel shows $[Ca^{2+}]_i$ measured in fura-2 loaded cells by using imaging microscopy. Depletion of intracellular stores with 1 μM TG activates CRAC in Jurkat T cells. Ca^{2+} entry is seen on addition of extracellular Ca^{2+} (n = 107). The resulting Ca^{2+} rise is blocked in cells preincubated with anti-CD95 Ab for 60 min (n = 91). Averaged responses are shown as bold traces, thin traces show representative individual cells. The bars display mean Ca^{2+} plateaus ± SEM in peripheral human T lymphoblasts after TG stimulation (n = 71, 62, and 84, respectively). Block of Ca^{2+} entry is already detected after 1 h incubation with anti-CD95 antibody and lasts for at least 18 h.

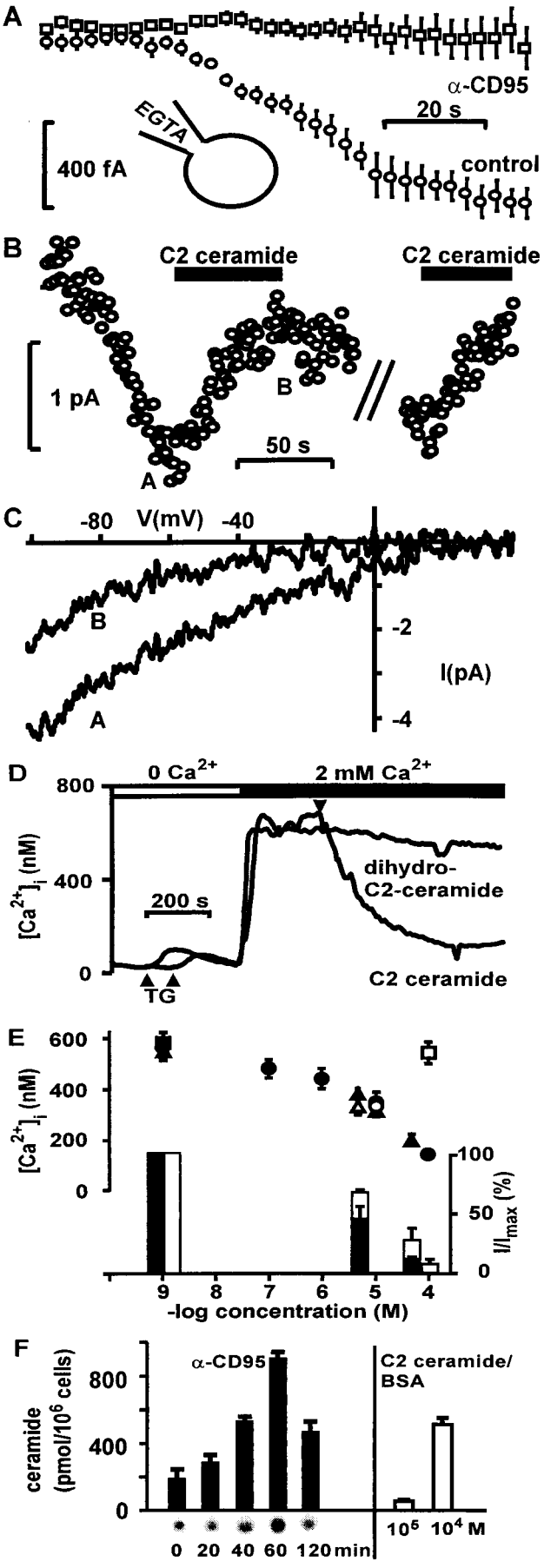

amount of Ca^{2+} released from intracellular stores in Ca^{2+}-free conditions after the application of TG was in good agreement with previous studies (21) and was not altered by CD95, excluding an effect on the Ca^{2+} content of intracellular stores or on the ability of TG to empty stores (Fig. 1*G*).

Store-Operated Ca^{2+} Channels Are Blocked by CD95 Stimulation. Because various factors like membrane depolarization can affect Ca^{2+} entry, current through CRAC was recorded in voltage-clamped single T cells by using the patch-clamp technique. The cytoplasm was dialyzed with EGTA after breaking into the whole-cell configuration. In control cells a typical, inwardly rectifying Ca^{2+} current developed because of the depletion of Ca^{2+} stores and the subsequent opening of store-operated CRAC (Fig. 2*A*). When cells were prestimulated with anti-CD95 for 1.5 h, development of the Ca^{2+} current was blocked (Fig. 2*A*). Acute addition of 100 ng/ml α-CD95 did not inhibit the current (not shown).

Ceramide and Sphingosine Block CRAC. During CD95 stimulation the lipid messenger ceramide is released by activated ASM (35). Ceramide can then be further metabolized to sphingosine. Acute addition of C2 ceramide, C6 ceramide, or sphingosine reversibly and dose-dependently blocked Ca^{2+} currents through CRAC in whole-cell patch-clamp recordings and Ca^{2+} entry (Fig. 2 *B–E*), whereas the inactive analogue dihydro-C2-ceramide had no effect (not shown). Polarizing the membrane voltage with 10 μM valinomycin did not affect inhibition by sphingolipids (Fig. 2*E*) or CD95 stimulation (not shown). Preincubation with C2 ceramide or sphingosine for up to 1 h also inhibited Ca^{2+} entry (not shown). Ceramide levels after a 5-min incubation with 100 μM ceramide/BSA corresponded well to the amount of ceramide generated 40–120 min after CD95 stimulation, in agreement with previously published results (Fig. 2*F*; refs. 22 and 23). We conclude that ASM metabolites mimic CD95-mediated inhibition of Ca^{2+} influx.

Fig. 2. Ca^{2+} entry through CRAC is blocked after CD95 stimulation and by ceramide. (*A*) Prestimulation with 100 ng/ml anti-CD95 Ab for 1.5 h inhibits CRAC activation in Jurkat T cells ($n = 6$). Whole-cell currents were measured directly by using the patch-clamp technique. After break-in, EGTA diffuses into the cytoplasm and depletes Ca^{2+} stores. An inward current through CRAC at −40 mV develops slowly in control cells. (*B*) Whole-cell patch-clamp recording from a single T cell. CRAC is reversibly blocked by 100 μM C2 ceramide/0.1% BSA ($n = 9$). (*C*) The current/voltage relation shows the typical, inwardly rectifying Ca^{2+} current through CRAC (*A*) that is blocked by ceramide (*B*). Current/voltage relations were obtained by using 200-ms voltage ramps and leak-subtracted. (*D*) The averaged time course of $[Ca^{2+}]_i$ in Jurkat cells shows inhibition of the TG-induced Ca^{2+} rise by 100 μM C2 ceramide/0.1% BSA, but not the inactive dihydro-C2-ceramide. The lower arrows indicate addition of TG, resulting in a transient Ca^{2+} rise because of the depletion of intracellular Ca^{2+} stores. The upper arrow indicates addition of ceramide. (*E, Upper*) Sphingosine (closed triangle, $n = 83$) and C2 ceramide (closed circle, $n = 75$), but not dihydro-C2-ceramide (open square, $n = 74$) inhibit Ca^{2+} influx dose-dependently. Valinomycin (10 μM) did not affect the block of Ca^{2+} entry by ceramide (open circle, $n = 47$) or sphingosine (open triangle, $n = 44$). Symbols indicate mean Ca^{2+} plateau values ± SEM of TG-treated Jurkat cells. (*Lower*) Sphingosine (filled bars, $n = 3$) inhibits CRAC more potently than C2 ceramide (open bars, $n = 6$). Whole-cell current was normalized to maximal Ca^{2+} current at −40 mV (see Fig. 2*A*). Similar results were obtained with C6 ceramide, yielding 55% inhibition at 10 μM (not shown, $n = 2$). All solutions contained 0.1% BSA. (*F*) Cellular ceramide levels after CD95 stimulation with 100 ng/ml α-CD95 in Jurkat T lymphocytes. Ceramide was measured with the diacylglycerol kinase assay. The ceramide spots were identified in TLC with autoradiography (*Lower*) and cut out, and activity was counted (filled bars). The open bars indicate binding of externally applied ^{14}C-labeled C2 ceramide to 10^6 Jurkat cells (5 min). All solutions contained 0.1% BSA. Representative for three experiments.

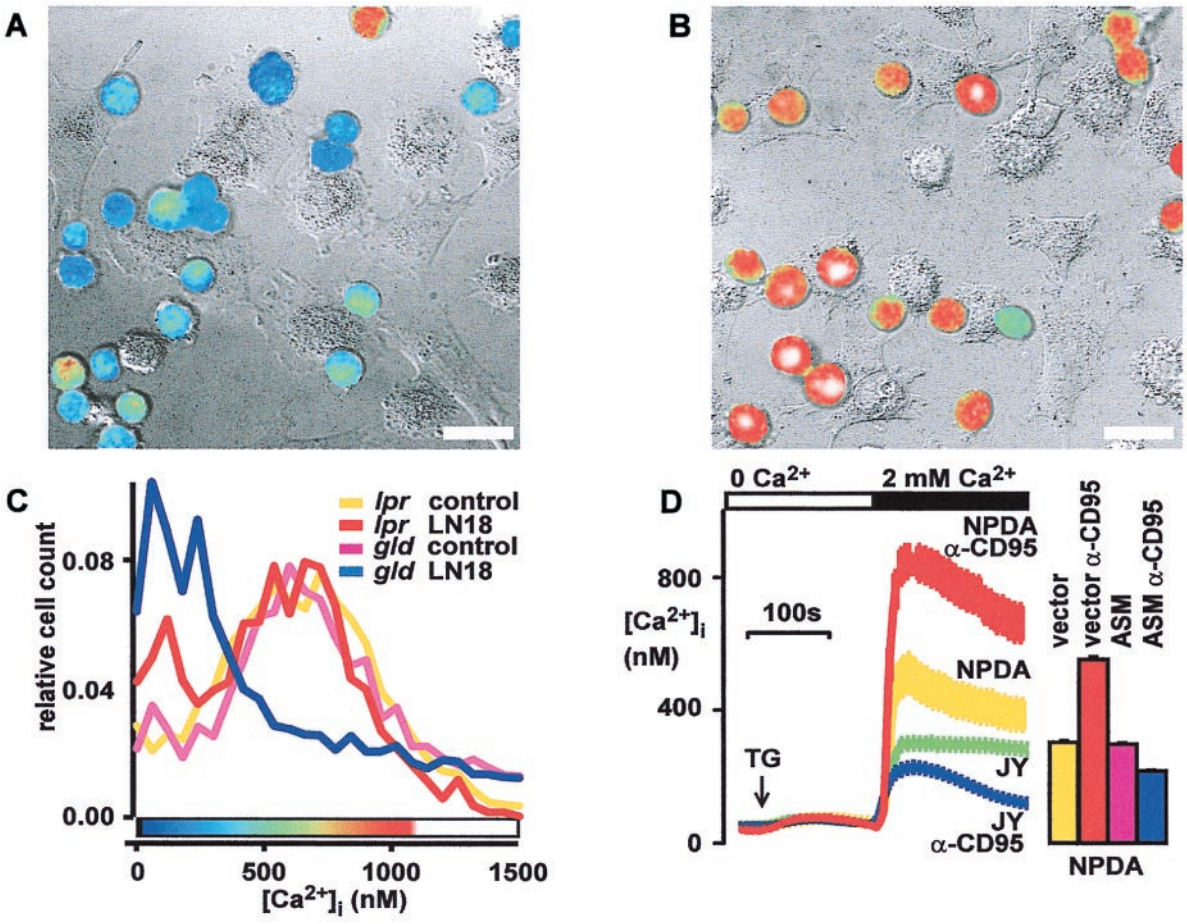

Fig. 3. CD95-induced block of store-operated Ca^{2+} entry requires CD95 and ASM. (*A*) Coculture with $CD95L^+$ glioblastoma (LN18) blocks store-operated Ca^{2+} entry in T lymphocytes. Similar results were obtained with a second $CD95L^+$ glioblastoma cell line (LN229). Fura-2 loaded Jurkat T cells were cocultured with $CD95L^+$ glioblastoma cells (LN18) for 1.5 h and Ca^{2+} entry was stimulated with TG (1 μM for 10 min). Pseudocolored ratio images of lymphocyte fluorescence encode intracellular free Ca^{2+} concentrations according to the color bar shown in *C*. Fluorescence ratio images of lymphocytes were digitally overlaid on transmission images obtained simultaneously with differential interference contrast. (Bars = 20 μm.) (*B*) Neutralization of CD95L with a CD95-Fc-fusion protein (3 μg/ml) prevents block of Ca^{2+} entry in T cells following coculture with LN18 tumor. (*C*) Ca^{2+} block requires a functional CD95 receptor. In *gld* thymocytes, coculture blocks Ca^{2+} entry. In contrast, in CD95-defective *lpr* thymocytes, influx of Ca^{2+} is not blocked. Frequency distribution histograms of $[Ca^{2+}]_i$ in single TG-stimulated thymocytes cocultured with LN18 tumor are shown. $[Ca^{2+}]_i$ was measured in 10^4 cells by using flow cytometry. The color bar shows the pseudocolor scale for panels *A* and *B*. (*D*) ASM-deficient cells respond to CD95 stimulation (100 ng/ml anti-CD95 Ab for 1 h) with an increased Ca^{2+} plateau, whereas the $[Ca^{2+}]_i$ rise evoked by TG in control cells is inhibited. Without CD95 triggering, the store-operated $[Ca^{2+}]_i$ rise is higher in ASM-deficient cells (NPDA) compared with control (JY) cells. $[Ca^{2+}]_i$ was measured with imaging microscopy in fura-2 loaded cells. Reconstitution of ASM into NPDA cells restores the Ca^{2+} block by CD95. Stimulated Ca^{2+} entry is increased after 1 h of CD95 stimulation in control-transfected NPDA cells. ASM transfection reverses this effect, leading to a block of Ca^{2+} entry by CD95. ASM transfection without CD95 stimulation has no effect on $[Ca^{2+}]_i$. Bars indicate mean $[Ca^{2+}]_i$ levels 5 min after TG stimulation in 10^4 transfected NPDA cells measured by flow cytometry. Two independent experiments were performed.

Block of Ca^{2+} Signals Requires CD95 and ASM. Human Jurkat T cells and murine thymocytes were then cocultured with CD95L-expressing glioblastoma cells for 1.5 h, resulting in a block of store-operated Ca^{2+} entry (Fig. 3*A*). Neutralizing CD95L by a CD95-Fc-fusion protein (Alexis Biotech, San Diego) prevented this block of Ca^{2+} entry (Fig. 3*B*), and coculture with CD95L-negative human foreskin fibroblasts did not inhibit Ca^{2+} entry (not shown). To prove the requirement of CD95 for this effect in a genetic model, CD95 or CD95L-deficient thymocytes from *lpr* or *gld* mice were employed. CD95L-deficient *gld* mice served as controls because they develop the same lymphoproliferative disease as *lpr* mice. $CD95L^+$ tumor cells blocked Ca^{2+} entry in thymocytes from CD95L-defective *gld* mice (Fig. 3*C*) as well as wild-type mice (not shown). In contrast, Ca^{2+} entry was not blocked in CD95-defective *lpr* thymocytes (Fig. 3*C*), demonstrating that CD95L blocks Ca^{2+} influx in T cells through CD95.

Next, we studied the involvement of ASM in CD95-mediated Ca^{2+} block by using NPDA B lymphoblasts that were lacking functional ASM. The ASM defect reversed the effect of CD95 on store-operated Ca^{2+} influx, whereas in wild-type B cells (JY or Daudi), Ca^{2+} entry was inhibited by CD95 (Fig. 3*D*). CD95 stimulation even increased TG-induced Ca^{2+} entry in NPDA cells (Fig. 3*D*). This result indicates the existence of CD95 signals in B cells that propagate Ca^{2+} influx, but they are normally masked by ASM-mediated inhibition of CRAC. Transfection of NPDA cells with an expression vector for ASM rescued the CD95 effect on Ca^{2+} signals in NPDA cells (Fig. 3*D*). These data demonstrate that ASM is required for CD95-mediated block of Ca^{2+} entry.

Block of Ca^{2+}-Dependent Lymphocyte Activation Signals. Activity of NFAT is known to be involved in the TCR-dependent IL-2 synthesis (24). TG strongly activated NFAT binding to the IL-2 promoter in nuclear extracts (Fig. 4*A*). CD95-AB, ceramide, or the immunosuppressant drug cyclosporin A blocked this binding activity (Fig. 4*A*).

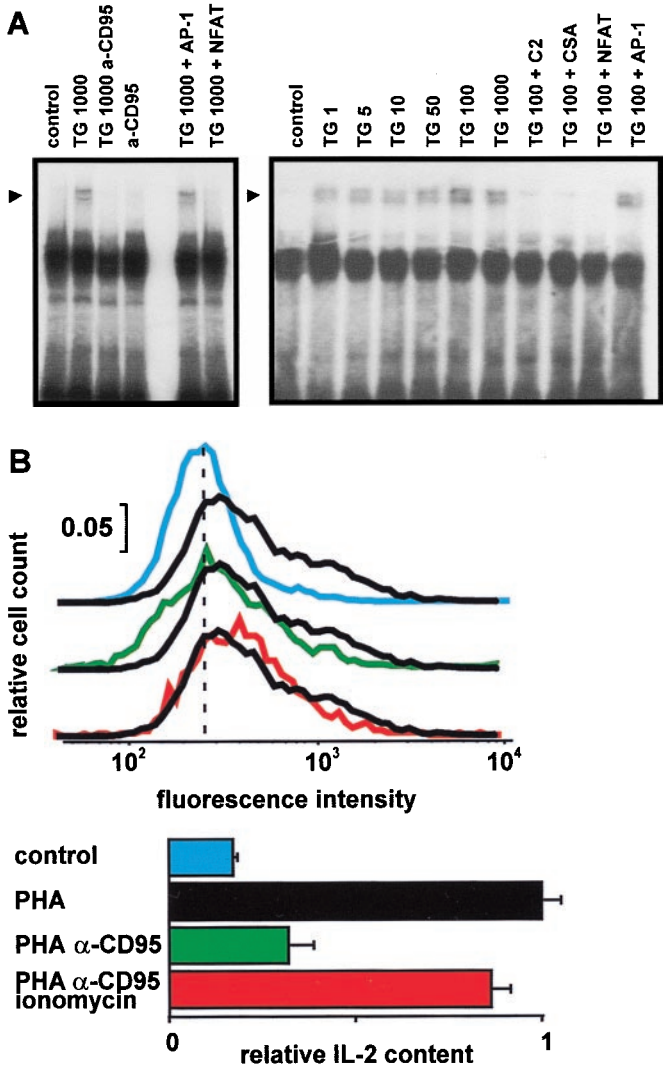

Fig. 4. CD95 stimulation inhibits NFAT activation and IL-2 synthesis. (*A*) Specific NFAT DNA-binding activity in nuclear extracts from Jurkat T cells is induced by TG and inhibited by 1 h preincubation with 100 ng/ml CD95 Ab. CD95 stimulation alone has no effect. Ca^{2+} influx was stimulated by application of TG for 20 min. Lanes labeled TG 1000 + AP-1 and TG 1000 + NFAT show excess cold competitor control oligonucleotides added to extracts from TG-stimulated cells to demonstrate specific binding. Numbers indicate TG concentrations in nM. NFAT activity is also blocked by C2 ceramide (100 μM) and cyclosporin A (CSA, 400 nM). Representative for three experiments. (*B*) Intracellular IL-2 was measured in viable, apoptosis-resistant cells by using flow cytometry. Jurkat T cells were stimulated for 18 h with a low dose of stimulating CD95 Ab (CH11, 100 ng/ml) followed by 5-h stimulation with PHA plus phorbol 12-myristate 13-acetate. IL-2 synthesis is inhibited in apoptosis-resistant cells. The Ca^{2+}-ionophore ionomycin (10 μM) restores IL-2 synthesis. (*Upper*) Histograms show distribution of fluorescence intensity with FITC-conjugated anti-IL-2. The dashed line indicates the mean of control intensities. Apoptotic cells were excluded by gating. To determine nonspecific binding, an irrelevant isotype-matched FITC-conjugated antibody was used (not shown). (*Lower*) The bar graph shows the mean intracellular IL-2-content ± SEM. Intensities were normalized and isotype fluorescence was subtracted. The results are representative for three independent experiments.

To distinguish between CD95-induced cell death and effects on lymphocyte function, we measured IL-2 synthesis in single apoptosis-resistant Jurkat T cells. Increased IL-2 synthesis was observed after TCR-stimulation (Fig. 4*B*). Upon a low-dose CD95-stimulation for 18 h (100 ng/ml CH11), 50% of the T cells survived. In this apoptosis-resistant population, IL-2 synthesis was blocked (Fig. 4*B*). As shown in Fig. 4*B*, the calcium ionophore ionomycin (10 μM) completely restored TCR-induced IL-2 synthesis despite CD95 stimulation. These results demonstrate that the block of Ca^{2+} channels via CD95 inhibits IL-2 transcription.

Discussion

In this paper, we describe block of store-operated Ca^{2+} entry through CRAC as a function of the CD95 receptor in lymphocytes. The block of Ca^{2+} entry by either CD95 stimulation or ASM-released lipid metabolites inhibits T cell activation signals, including Ca^{2+} influx, NFAT activation, and IL-2 production. Thus, CD95 represents a receptor negatively regulating T cell Ca^{2+} channels. Block of Ca^{2+}-dependent T cell signals might be significant for understanding CD95-mediated immune suppression. Manipulating CD95-induced suppression of T cell activation could be beneficial for therapeutic strategies to prevent tumor immune evasion, to increase the efficacy of antitumor vaccines, and to aim at specific immune suppression in organ transplantation.

Store-operated or calcium-release-activated Ca^{2+} channels are opened by any manipulation reducing the endoplasmic reticulum Ca^{2+} content, i.e., by using either inositoltrisphosphate/Ca^{2+} chelators or blockers of the Ca^{2+} reuptake into the endoplasmic reticulum (2, 25). In this paper, Ca^{2+} influx and Ca^{2+}-dependent signals were blocked after CD95-stimulation whether we activated store-operated Ca^{2+} influx by stimulation of the TCR, by direct depletion of stores with TG, or with intracellular EGTA. TG has been shown to activate the same CRAC as TCR-stimulation by antigen (26). We used TG to bypass TCR signals upstream of the endoplasmic Ca^{2+} store and, thus, to specifically assay the influence of CD95 stimulation on CRAC.

Several signals inhibiting store-operated Ca^{2+} entry have been described. In B lymphocytes, negative signaling through FcγRII receptors involves inhibition of Ca^{2+} influx (27). CRAC is inhibited in mast cells via protein kinase C (28). Inhibition of Ca^{2+} entry by sphingomyelinase products has been observed in T cells, mast cells, and thyroid cells (29–31). Mathes *et al.* (30) analyzed in detail the effects of different sphingolipids on mast cells. The slow accumulation of lipids in the membrane assayed by membrane capacitance corresponded well to the time course and degree of inhibition. In mast cells, the ceramide metabolite sphingosine inhibited CRAC more potently and faster than C2 ceramide, and nerve growth factor inhibited CRAC currents rapidly (30). In a thyroid cell line, tumor necrosis-factor α, bacterial sphingomyelinase, and C2 as well as C6 ceramide inhibited Ca^{2+} influx (31).

In our study we genetically manipulated ASM, showing that this enzyme is indispensable for inhibition of CRAC by CD95. Like in mast cells, sphingosine that can be cleaved from ceramide by ceramidase was more potent than C2 ceramide. In contrast to mast cells, but similar to thyroid cells, C6 ceramide inhibited lymphocyte CRAC (30, 31). Whereas nerve growth factor acutely inhibited CRAC in mast cells (30), CD95 in lymphocytes had to be stimulated for 1 h, possibly indicating a slower accumulation of sphingolipids. Interestingly, the metabolite sphingosine-phosphate, which stimulates proliferative EDG receptors, does not inhibit CRAC in mast cells (30). To pinpoint the exact lipid metabolite(s) downstream of ASM or their putative target(s), genetic manipulation of ceramidase as well as identification of the CRAC protein will be required.

Previously, CD95 has been suggested to inhibit TCR signals, because TCR-induced anergy is lacking in T cells from *lpr* mice (32) and costimulation of CD95 and the TCR can inhibit release of inositoltrisphosphate in human lymphoblasts (33). In the study performed by Kovacs and Tsokos (33), store-operated Ca^{2+} entry activated by TG was not inhibited by CD95 crosslink-

ing, but α-CD3-induced Ca^{2+} entry was reduced; however, Ca^{2+} release was not clearly separated from influx and Ca^{2+} assays were not calibrated. By using store depletion in Ca^{2+}-free conditions with subsequent readdition of Ca^{2+}, we observed a block of store-operated Ca^{2+} entry in human T lymphoblasts after CD95 stimulation. Although our data do not exclude additional effects of CD95 on TCR signals upstream of the Ca^{2+} store, the rescue of TCR-stimulated IL-2 synthesis by raising $[Ca^{2+}]_i$ with ionomycin demonstrates that the block of CRAC is sufficient for inhibition of Ca^{2+}-dependent TCR signals. Furthermore, the unchanged Ca^{2+} release points to an inhibition of TCR signals by CD95 downstream of endoplasmic reticulum Ca^{2+} stores.

CD95 is an important suppressor of the immune response and has so far been thought to act by the induction of lymphocyte apoptosis. Rejection of transplanted melanoma cells is increased in *lpr* compared with *gld* mice (9), and transplanted testicular tissue from *gld* mice is rejected more rapidly than wild-type tissue (34), indicating a role of CD95 for immune tolerance to transplanted malignant and normal cells. The block of Ca^{2+} channels via CD95 could account for observations implying CD95-mediated impairment of lymphocyte function. Mice inoculated with a CD95L-expressing tumor show CD95-mediated defects in T and B lymphocyte function (14). Interestingly, inhibition of Ca^{2+} signals has been observed in T lymphocytes from glioblastoma patients (12). Our observation of CD95-induced Ca^{2+} block may provide a molecular basis for these observations. The CD95-induced block of Ca^{2+} signals described here could alter lymphocyte function before or even in the absence of apoptosis. Because several members of the nerve growth factor/tumor necrosis factor receptor family share the potential to activate ASM and inhibit CRAC (30, 31), the pathway described here may represent a general means to suppress Ca^{2+}-dependent lymphocyte activation signals.

We thank Drs. A. Fontana, K.-U. Hartmann, H.-G. Rammensee, and C. Dehio for valuable reagents and discussions. This work was supported in part by grants from the Deutsche Forschungsgemeinschaft (Le792/3-1, Gu335/2-2, and La315/4-2), the Fortüne program (333, to C.B.), the Scheel Foundation (to A.L.-W., E.G., and C.B.), and Interdisziplinäres Zentrum für Klinische Forschung (IIB9, to E.G. and A.L.-W.).

1. Qian, D. & Weiss, A. (1997) *Curr. Opin. Cell Biol.* **9,** 205–212.
2. Zweifach, A. & Lewis, R. S. (1993) *Proc. Natl. Acad. Sci. USA* **90,** 6295–6299.
3. Negulescu, P. A., Shastri, N. & Cahalan, M. D. (1994) *Proc. Natl. Acad. Sci. USA* **91,** 2873–2877.
4. Lewis, R. S. & Cahalan, M. D. (1995) *Annu. Rev. Immunol.* **13,** 623–653.
5. Van Parijs, L. & Abbas, A. K. (1998) *Science* **280,** 243–247.
6. Griffith, T. S., Brunner, T., Fletcher, S. M., Green, D. R. & Ferguson, T. A. (1995) *Science* **270,** 1189–1192.
7. French, L. E., Hahne, M., Viard, I., Radlgruber, G., Zanone, R., Becker, K., Muller, C. & Tschopp, J. (1996) *J. Cell Biol.* **133,** 335–343.
8. Strand, S., Hofmann, W. J., Hug, H., Muller, M., Otto, G., Strand, D., Mariani, S. M., Stremmel, W., Krammer, P. H. & Galle, P. R. (1996) *Nat. Med.* **2,** 1361–1366.
9. Hahne, M., Rimoldi, D., Schroter, M., Romero, P., Schreier, M., French, L. E., Schneider, P., Bornand, T., Fontana, A., Lienard, D., *et al.* (1996) *Science* **274,** 1363–1366.
10. Klas, C., Debatin, K. M., Jonker, R. R. & Krammer, P. H. (1993) *Int. Immunol.* **5,** 625–630.
11. Peter, M., Kischkel, F. C., Scheuerpflug, C. G., Medema, J. P., Debatin, K. M. & Krammer, P. H. (1997) *Eur. J. Immunol.* **27,** 1207–1212.
12. Morford, L. A., Elliott, L. H., Carlson, S. L., Brooks, W. H. & Roszman, T. L. (1997) *J. Immunol.* **159,** 4415–4425.
13. Staveley-O'Carroll, K., Sotomayor, E., Montgomery, J., Borrello, I., Hwang, L., Fein, S., Pardoll, D. & Levitsky, H. (1998) *Proc. Natl. Acad. Sci. USA* **95,** 1178–1183.
14. Arai, H., Chan, S. Y., Bishop, D. K. & Nabel, G. J. (1997) *Nat. Med.* **3,** 843–848.
15. Newton, K., Harris, A. W., Bath, M. L., Smith, K. G. C. & Strasser, A. (1998) *EMBO J.* **17,** 706–718.
16. Zhang, J. K., Cado, D., Chen, A., Kabra, N. H. & Winoto, A. (1998) *Nature* **392,** 296–300.
17. Weller, M., Weinstock, C., Will, C., Wagenknecht, B., Dichgans, J., Lang, F. & Gulbins, E. (1997) *Cell. Physiol. Biochem.* **7,** 282–288.
18. Grassmé, H., Gulbins, E., Brenner, B., Ferlinz, K., Sandhoff, K., Harzer, K., Lang, F. & Meyer, T. F. (1997) *Cell* **91,** 605–615.
19. Novak, E. J. & Rabinovitch, P. S. (1994) *Cytometry* **17,** 135–141.
20. Thastrup, O., Cullen, P. J., Drobak, B. K., Hanley, M. R. & Dawson, A. P. (1990) *Proc. Natl. Acad. Sci. USA* **87,** 2466–2470.
21. Premack, B. A., McDonald, T. V. & Gardner, P. (1994) *J. Immunol.* **152,** 5226–5240.
22. Hannun, Y. A. (1996) *Science* **274,** 1855–1859.
23. Gulbins, E., Bissonnette, R., Mahboubi, A., Martin, S., Nishioka, W., Brunner, T., Baier, G., Baier-Bitterlich, G., Byrd, C., Lang, F., *et al.* (1995) *Immunity* **2,** 341–351.
24. Shaw, J. P., Utz, P. J., Durand, D. B., Toole, J. J., Emmel, E. A. & Crabtree, G. R. (1988) *Science* **241,** 202–205.
25. Hoth, M. & Penner, R. (1992) *Nature (London)* **355,** 353–356.
26. Aussel, C., Marhaba, R., Pelassy, C. & Breittmayer, J. P. (1996) *Biochem. J.* **313,** 909–913.
27. Choquet, D., Partiseti, M., Amigorena, S., Bonnerot, C., Fridman, W. H. & Korn, H. (1993) *J. Cell Biol.* **121,** 355–363.
28. Parekh, A. B. & Penner, R. (1995) *Proc. Natl. Acad. Sci. USA* **92,** 7907–7911.
29. Breittmayer, J. P., Bernard, A. & Aussel, C. S. O. (1994) *J. Biol. Chem.* **269,** 5054–5058.
30. Mathes, C., Fleig, A. & Penner, R. (1998) *J. Biol. Chem.* **273,** 25020–25030.
31. Törnquist, K., Malm, A.-M., Pasternack, M., Kronquist, R., Björklund, S., Tuominen, R. & Slotte, J. P. (1999) *J. Biol. Chem.* **274,** 9370–9376.
32. Bossu, P., Singer, G. G., Andres, P., Ettinger, R., Marshak-Rothstein, A. & Abbas, A. K. (1993) *J. Immunol.* **151,** 7233–7239.
33. Kovacs, B. & Tsokos, G. C. (1995) *J. Immunol.* **155,** 5543–5549.
34. Bellgrau, D., Gold, D., Selawry, H., Moore, J., Franzusoff, A. & Duke, R. C. (1995) *Nature (London)* **377,** 630–632.
35. Cifone, M. G., De-Maria, R., Roncaioli, P., Rippo, M. R., Azuma, M., Lanier, L. L., Santoni, A. & Testi, R. (1994) *J. Exp. Med.* **180,** 1547–1552.